Perspective

Cite This: Biomacromolecules 2019, 20, 1135−1145

pubs.acs.org/Biomac

Active, Autonomous, and Adaptive Polymeric Particles for Biomedical Applications

Shauni Keller,[‡] B. Jelle Toebes,[‡] and Daniela A. Wilson*

Institute of Molecules and Materials, Radboud University, Heyendaalseweg 135, 6525 AJ Nijmegen, The Netherlands

ABSTRACT: Nature's motors are complex and efficient systems, which are able to respond to many different stimuli present in the cell. Nanomotors for biomedical applications are designed to mimic nature's complexity; however, they usually lack biocompatibility and the ability to adapt to their environment. Polymeric vesicles can overcome these problems due to the soft and flexible nature of polymers. Herein we will highlight the recent progress and the crucial steps needed to fabricate active and adaptive motor systems for their use in biomedical applications and our approach to reach this goal. This includes the formation of active, asymmetric vesicles and the incorporation of a catalyst, together with their potential in biological applications and the challenges still to overcome.

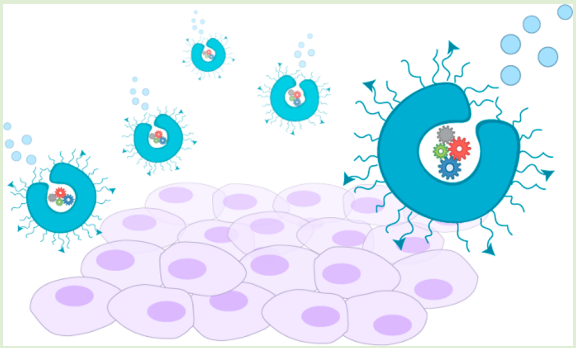

1. INTRODUCTION

Biological motors, such as ribosomes,[1] kinesins,[2] and ATP synthase,[3] are essential natural machines that perform their functions with supreme efficiency. Many scientists have tried to understand and mimic these structures by creating various synthetic micro- and nanosized motors, in particular those that lead to translational motion. Combining structural design with motion has led to many successful constructs, such as molecular motors,[4−6] switches,[7] ratchets,[8] bimetallic nanorods,[9−13] Janus capsules,[14,15] and shuttles.[16,17] The specific requirements of each motor depend on their application and functional design, yet, asymmetry plays an important role in the design, together with the incorporation of a catalyst that can convert chemical energy into motion. To mimic biological motors, the system should be adaptive and made from soft and biodegradable materials. This ensures that the motor can feel its environment and respond accordingly, so that it is able to actively perform the task it was designed for. So far, the majority of research has focused on creating artificial motors that are based on metal catalysts or metal surfaces and are therefore not compatible for biomedical applications. The challenge is to design nanomotors made of soft materials, which are adaptive and fully biocompatible and/or biodegradable. Therefore, it is necessary to consider not only the structural design but also the construction approach.

The two main approaches for the formation of micro- and nanostructures are top-down and bottom-up, although, increasingly hybrid methods are used as well, which combine advantages of both methods. With the top-down approach, larger structures or patterns are reduced to nanoscale dimensions. The methods that are mostly used are subtractive and additive lithography techniques, such as etching, electrodeposition, and sputtering, or molding processes, such as PDMS printing. Fabrication using a top-down approach is straightforward and cheap; however, the scale up production is difficult to achieve and it faces size limitations when going for even smaller designs. The first nano- and micromotors have been created using these techniques.[18−21] The bottom-up approach starts with molecular building blocks that are used to build up the final structure, often involving synthesis or self-assembly. The bottom-up approach is more versatile in design and choice of materials. With this method the smallest structures can be made, for instance the well-known molecular motors from the Feringa group.[22−24] Lately, several examples of nanomotors are published that combine the top-down and bottom-up approach, such as the fabrication of ordered arrays of functional nanotubes,[25] directed self-assembly of polymers by patterned templates,[26] and layer-by-layer deposition to form multilayer Janus capsules.[27]

However, limited examples exist of motors created solely by bottom-up approaches.[28,29] Our lab has reported bottom-up self-assembly of micro- and nanomotors from different polymers.[17,30−33] The supramolecular approach to develop nanomotor carriers for biomedical applications is the main inspiration for our group. Designing soft, biocompatible carriers has a wide range of implications, not only from the applications point of view, but also from the perspective of mimicking and consequent understanding of such fascinating structures. In this Perspective, the supramolecular paths to form asymmetric morphologies are discussed that form the foundation of our self-propelling structures. In the following subsections, we focus on the development of asymmetric structures into nanomotors by incorporating a catalyst and their potentials for biomedical applications by showing their adaptive abilities, cellular uptake and release of drug molecules. Comprehensive reviews focused on nano- and micromotors

Received: November 20, 2018
Revised: December 20, 2018
Published: December 21, 2018

DOI: 10.1021/acs.biomac.8b01673
Biomacromolecules 2019, 20, 1135−1145

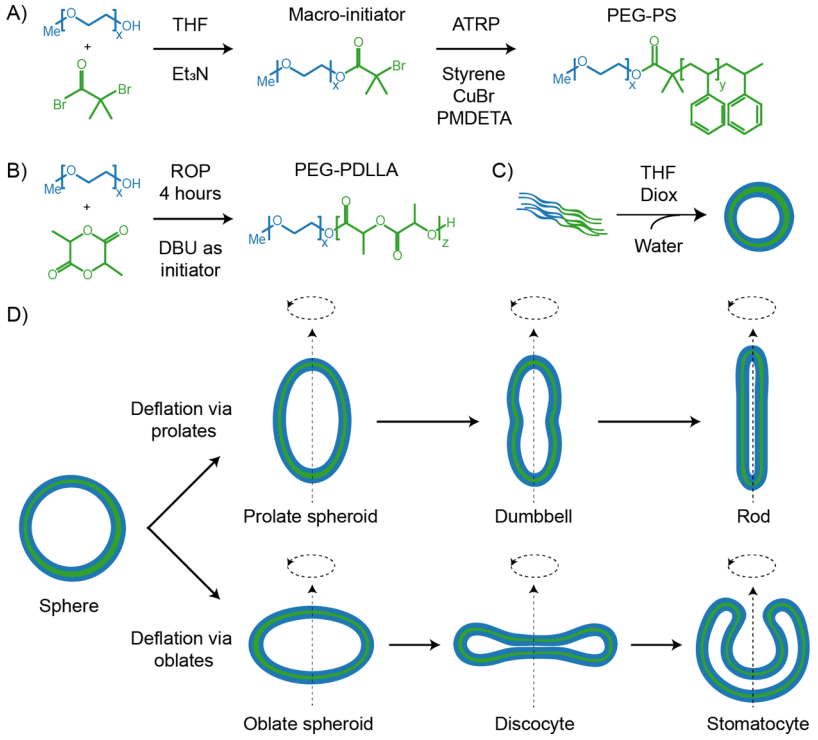

Figure 1. Synthesis and self-assembly of block copolymers. (A) Synthesis of poly(ethylene glycol)-polystyrene via atom transfer radical polymerization (ATRP). (A) Synthesis of poly(ethylene glycol)-*b*-poly(D,L-lactide) via ring opening polymerization (ROP). (C) Self-assembly of amphiphilic block copolymers in organic solvent by addition of water. (D) Shape transformation pathways of spherical polymersomes. Deflation occurs via prolate or oblate structures. Dashed arrows represent the axis of symmetry.

and their applications,[34−36] molecular motors,[37,38] and on nanoreactors[39−41] and will not be discussed here. Instead, we specifically focus on self-assembled polymeric motors and our approach from fabrication to application.

2. SHAPE

The first factor to consider while designing autonomous particles is their shape. Asymmetry, either in catalyst distribution or in shape, is required to obtain autonomous motion. Here we focus on the design of asymmetric shapes for our micro- and nanomotor.

Polymersomes are bilayered polymeric vesicles made from amphiphilic block copolymers comprising hydrophobic and hydrophilic covalently linked chains (Figure 1A,B). In aqueous media, these block copolymers spontaneously self-assemble into spherical vesicles (Figure 1C).[17,30] Thereby, three different compartments are created; an inner aqueous lumen, a hydrophobic membrane and a hydrophilic outer surface. During polymersome formation, cargo can be captured inside the lumen, which is shielded from potentially unfavorable environments in biological settings.[30,42] This allows the formation of nanocarriers or nanoreactors for various applications, such as drug delivery,[43] imaging[44] or mimics of life-like systems.[45] Polymersomes show increased stability and membrane integrity compared to liposomes, due to their relatively thick membrane and are therefore used as alternative carriers.[17,32] While a thick membrane allows them to tolerate changes in the environment, their morphology can be re-engineered and reshaped upon different stimuli. The shape transformation of spherical polymersomes in response to various external stimuli, such as pH,[46,47] osmotic pressure,[48,49] temperature,[50,51] chemical composition of the membrane[52,53] and magnetic fields[54,55] has been studied. Yet, it is important to highlight that the polymersome properties, i.e., size, surface charge, rigidity, and permeability, depend on their building blocks.[56−58] For the hydrophilic part of the block copolymer often poly(ethylene glycol) (PEG) is implemented, due to its stealth-like behavior. Although PEG is not biodegradable, it is proven to be biocompatible.[59,60] As hydrophobic block, various polymers have been used,[61−63] i.e., polybutadiene (PBD),[64] polystyrene (PS),[65] poly(ε-caprolactone) (PCL),[66] and polylactide (PLA),[67] depending on their application. For instance, polybutadiene has a glass transition temperature (T_g) below room temperature, which makes the polymersomes quite flexible and suitable for drug release. On the other hand, polystyrene has a high T_g, which creates a rigid amorphous membrane when the organic solvent is removed, due to tight packing of the benzene rings (Figure 1A).[68] These characteristics are useful for shape transformation of polymersomes, as different (intermediate) morphologies can be obtained. However, neither polybutadiene nor polystyrene are biodegradable, so for biomedical applications alternatives are required. Polylactide is a good candidate, as it is biodegradable and has comparable properties to polystyrene, i.e., a relatively high T_g and similar Hildebrand solubility parameters (Figure 1B).

Creating various shapes from spherical polymersomes is exciting and important for many different applications. Therefore, understanding the fundamentals of the shape transformations is key. Spherical polymersomes can deflate via two distinct pathways defining the final morphology; prolates (rod-like structures) or oblates (disc-like structures)[49] (Figure 1D). The out-of-equilibrium situations that forces spherical polymersomes to deflate into different morphological

DOI: 10.1021/acs.biomac.8b01673
Biomacromolecules 2019, 20, 1135−1145

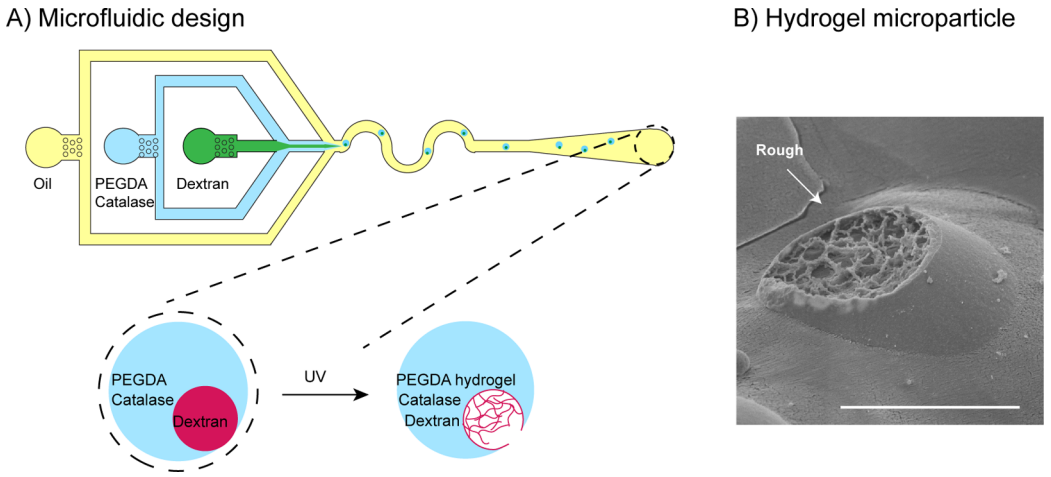

Figure 2. (A) Microfluidic design for the generation of droplet-in-droplet morphologies of poly(ethylene glycol) diacrylate (PEGDA) and dextran. The dextran phase templates the asymmetric shape, upon polymerization of PEGDA it will partly diffuse inside the gel resulting in a rough inner surface. (B) Cryo-scanning electron microscopy (cryo-SEM) image of the microparticle showing the rough inner surface. Scale bar corresponds to 10 μm. Reproduced from ref 33 with permission from John Wiley and Sons. Copyright 2018 Wiley-VCH Verlag GmbH & Co. KGaA, Weinheim.

structures can be explained in terms of bending energy (eq 1).[49,69]

$$E_b = \frac{k}{2}\oint(2C - C_0)^2 dA \quad (1)$$

In this equation k is the bending rigidity constant (which depends on material properties), C is the mean surface curvature, and C_0 stands for the spontaneous surface curvature. When an external stimulus is applied to a flexible membrane, a positive or negative surface curvature is induced, thereby influencing the bending energy. A positive bending energy will lead to the formation of prolate morphologies, whereas a negative bending energy leads to the formation of oblate morphologies. The hydrophilic and hydrophobic parts of the polymersome largely influence the surface charge, temperature sensitivity, rigidity and permeability and thereby affect the shape change process.[56−58] For example, introducing an osmotic shock to spherical poly(ethylene glycol)-*b*-poly(D,L-lactide) (PEG-*b*-PDLLA) polymersomes allows shape transformation into elongated nanotubes (prolates), whereas poly(ethylene glycol)-polystyrene (PEG-*b*-PS) showed stomatocyte morphologies (oblates) under similar conditions.[48,49] However, careful tuning of the conditions makes it possible to create nanorods and nanotubes of PEG-*b*-PS[49] or stomatocytes of PEG-*b*-PDLLA.[70] By adding high amounts of PEG (M_w 2000) to spherical polymersomes it is even possible to create stomatocyte in stomatocyte structures.[71] The final shape is not only important for their function but also for their application and communication to the environment. For example, structures with high aspect ratio have more interaction sites, leading to enhanced particle uptake by cells through multivalency.[72]

Polymersomes assembled from PEG-*b*-PS have a flexible and responsive bilayer membrane in the presence of plasticizing organic solvents and are rigid and nonresponsive in water due to the tightly packed glassy hydrophobic polystyrene blocks in their membranes. Once the plasticizing solvent is completely removed, the kinetically driven process of membrane folding stops due to vitrification of the membrane. The shape transformation can therefore also be stopped at any moment during the shape transformation process by adding excess of water, quenching the (intermediate) structures and forcing the system in a kinetically trapped state.[73] These properties enabled the shape transformation of spherical vesicles into bowl-shaped stomatocytes via disc morphologies by dialyzing against water (Figure 1D).[30] However, small amounts of organic solvents or additives in the sample leave the membrane slightly flexible and permeable, allowing solvent exchange from the inner lumen and outside environment. This can result in a metastable configuration, where the system slowly relaxes to a more stable configuration.[73] For instance, spherical PEG-PS polymersomes can deflate in a mixture of water and organic solvent to prolate structures and subsequently inflate back to spheres after multiple days. By adding 50% (v/v) water, a slight osmotic pressure is generated over the spherical polymersomes, causing an outflow of organic solvent. The polymersomes will form a prolate morphology to lower the osmotic pressure at the expense of the bending energy. When the organic solvent is not removed, it acts as plasticizer, allowing water to flow back in slowly, relieving the bending energy. This results in the inflation of the prolates to the more stable spherical polymersomes.[49]

The method in which the organic solvent is removed completely, is named the "solvent switch" method, as the plasticizing solvent is switched for water, rigidifying the final polymersome morphology. Another approach is the "reverse addition" method, in which glassy stomatocytes are reversibly plasticized and made flexible when dialyzed in a mixture of organic solvent and water.[30] Depending on the time of exposure to the plasticizer, different morphologies are obtained, such as ellipsoids and kippah structures.[74] When the same reverse dialysis method was applied to rigid glassy polymersomes, stomatocyte morphologies were obtained with different sizes of their openings, depending on the time of dialysis and the mixture and composition of water and organic solvent.[42] The desired morphologies could also be quenched by vitrifying the membrane in water, allowing reshaping of existing polymersome morphologies. The drawback of this method, however, is the limited control in the size of the opening of the stomatocytes due to the increased flexibility of the membrane during the reverse dialysis. A third method was developed to provide a mild methodology for shape trans-

DOI: 10.1021/acs.biomac.8b01673
Biomacromolecules 2019, 20, 1135−1145

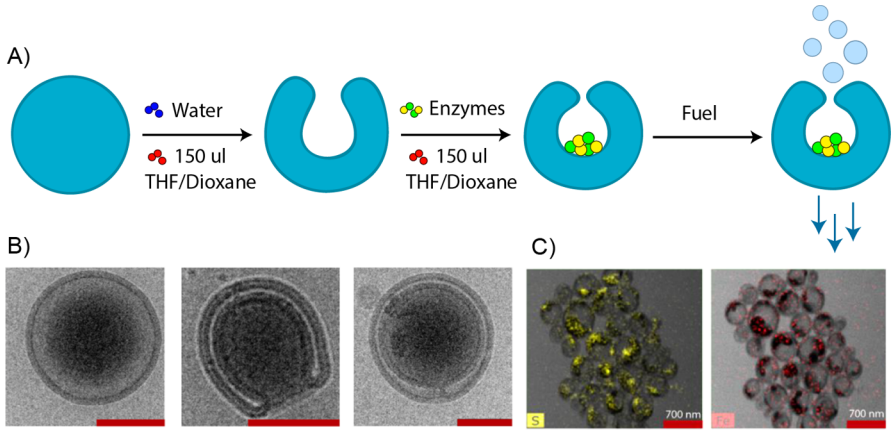

Figure 3. (A) Incorporation of enzymes inside the stomatocyte cavity. Encapsulation is performed under mild conditions to minimize contact of the enzymes with organic solvent. Small amounts of organic solvent are added to form and close the opening of the stomatocyte. When fuel is added, the entrapped enzymes produce water and oxygen to propel the nanomotor forward. (B) Cryo-transmission electron microscopy (cryo-TEM) pictures of spherical polymersomes, open and closed stomatocytes. Scale bars correspond to 200 nm. (C) TEM coupled with energy dispersive X-ray spectroscopy (EDX) showing the mapping of iron (Fe) and sulfur (S), specific for enzymes and the localization inside the stomatocyte cavity. Adapted with permission from ref 42. Copyright 2016 American Chemical Society.

formation in biological setting for encapsulation of proteins and enzymes. Large amounts of solvent can damage these complex structures, as will be discussed in later sections, thus the "solvent addition" method was introduced.[42] In this method, small amounts of solvent are added to spherical PEG-PS polymersomes to introduce shape transformation based on fast osmotic stress generation over the glassy PS membrane. Upon addition of less than 25% (v/v) of solvent, a shape transformation from spherical polymersomes to large opening stomatocytes was observed. Adding more aliquots led to a decrease of the stomatocyte neck size, to the extent that virtually closed stomatocytes were obtained. At any stage of this cycle, organic solvent could be removed and water could be added to capture the stomatocyte structure with controlled opening. The stomatocyte structure provides both asymmetry as well as a protected inner cavity, thus offering a lot of interesting possibilities, especially for nanomotors or nano-reactor applications.

Recently, we designed a micromotor to mimic the stomatocyte shape at the microscale.[33] Because such micro-sized particles are easier to visualize, we hoped to learn more about their behavior and correlate this to the nanoscale. Although this is a nice strategy to mimic the shape of the stomatocyte nanoparticles, the microparticle is made from a completely different material; a cross-linked gel. The formation of asymmetric particles is based on the phase separation of two polymeric solutions, which are poly(ethylene glycol)diacrylate (PEGDA) and dextran. In a microfluidic chip, a droplet-in-droplet system is generated containing dextran in PEGDA in oil, which is the continuous phase and ensures emulsification of the PEGDA/dextran droplets. After collection from the chip, the PEGDA phase can be specifically polymerized due to the diacrylate functionality. The dextran phase is added as a template to provide the asymmetry in the particle. Upon polymerization of PEGDA, it will partly diffuse inside the gel and ensures a rough inner surface (Figure 2).

In the section below, the incorporation of a catalyst in the stomatocytes is described, including a metal catalyst, which decomposes hydrogen peroxide into water and propelling oxygen, and an enzyme couple catalyst that uses glucose as fuel.

3. AUTONOMOUS SYSTEMS

The first stomatocyte nanomotors were created by the encapsulation of platinum nanoparticles inside their cavity during the shape transformation via a process called "artificial endocytosis".[30] Interestingly, when large particles (100 nm) were used for encapsulation, size and shape of the stomatocyte cavity were accordingly affected due to a possible templating effect from the particle. Platinum is a known catalyst for the decomposition reaction of hydrogen peroxide into water and oxygen, which can escape through the opening of the stomatocytes, propelling it forward. The state-of-art design was conceptually an important milestone for developing new stomatocyte biohybrid motors, using enzymes instead of platinum as engines and utilizing biofuels instead of hydrogen peroxide for propulsion. For this purpose, the "solvent addition" methodology was developed to protect the enzymes from denaturation. Enzymes were first mixed with open neck stomatocytes and subsequently, the neck was closed by adding small amounts of organic solvent. This process led to the encapsulation of the enzymes while their denaturation was prevented, forming a hybrid polymeric supramolecular nanomotor (Figure 3).[42] We encapsulated the well-known enzyme cascade glucose oxidase (GOx) and catalase (Cat) in the stomatocytes to break down glucose. GOx catalyzes the oxidation of glucose to gluconolactone and H_2O_2, which is decomposed by Cat into water and propelling oxygen. The stomatocytes encapsulating both enzymes showed propulsion at biological relevant glucose concentration (5 mM) and continued moving in the presence of trypsin, a proteolytic enzyme known to inhibit enzymes activity.

4. ADAPTIVE NANOMOTORS

The next step, a far more challenging task, is to make adaptive systems that can interact and respond to their environment. Earlier attempts to achieve this adaptability by control over motion included disassembly of the complete system[75] and chemical inhibition of the catalytic process,[76] which led to the complete loss of motion without the possibility of restarting. Inhibition of the catalytic process involves adding more chemicals to the system, increasing complexity and decreasing

DOI: 10.1021/acs.biomac.8b01673
Biomacromolecules 2019, 20, 1135−1145

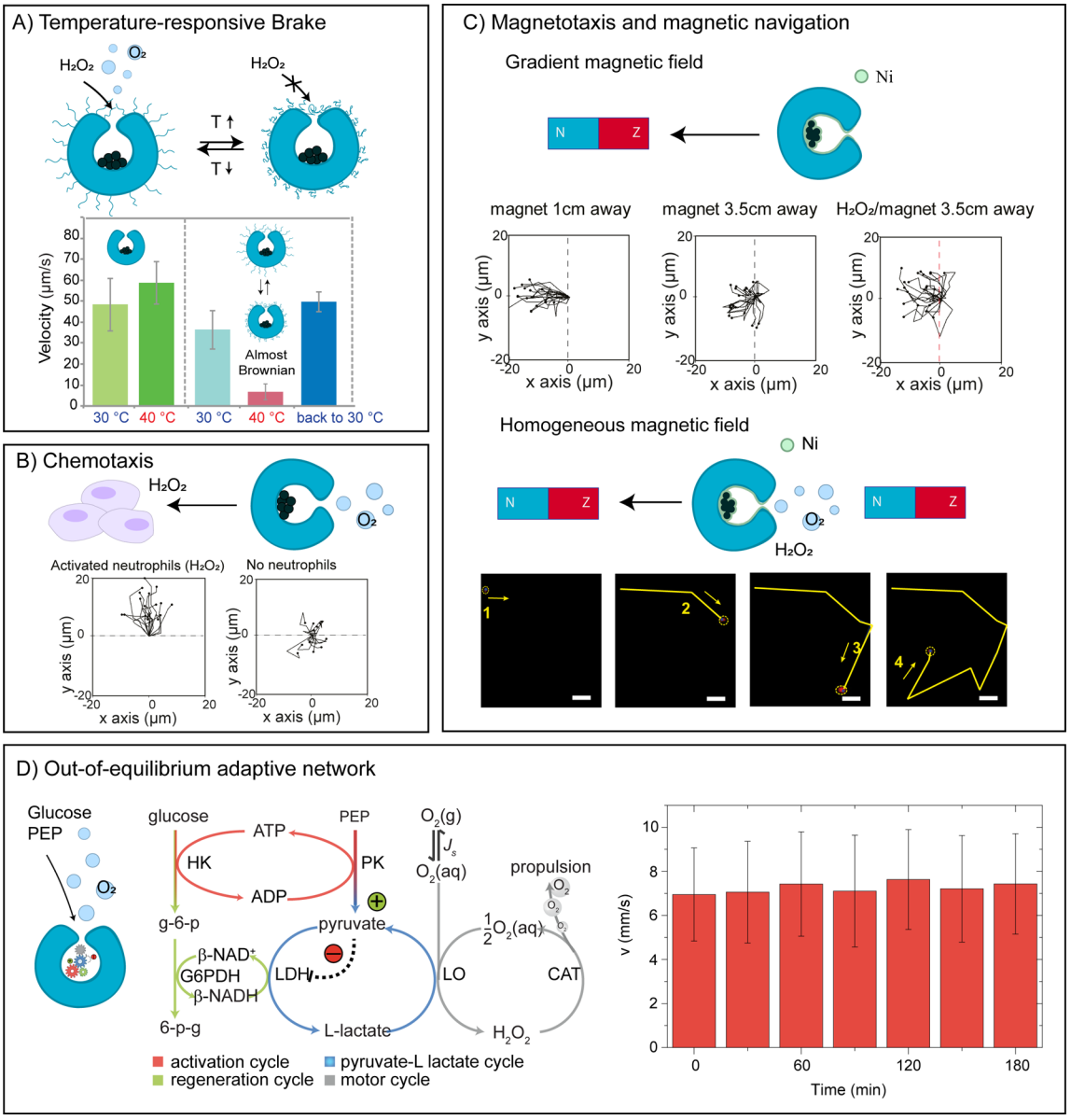

Figure 4. Schematic overview of adaptive supramolecular nanomotor systems. (A) Temperature-responsive poly(*N*-isopropylacrylamide) PNIPAM brush as reversible brake. At 30 °C, the PNIPAM is hydrophilic, allowing access of fuel to the stomatocyte cavity; however, at 40 °C the PNIPAM becomes hydrophobic, which induces a collapsed state denying access to fuel and ceasing nanomotor motion. Adapted by permission from Springer Nature, ref 77. Copyright 2017 Macmillan Publishers Limited, https://www.nature.com/nchem/. (B) Because of the chemotactic nature of the nanomotors, they move toward higher concentration of fuel. The graph left shows highly directional motion along the fuel gradient, while the graph right in absence of fuel shows no directionality at all. Adapted from ref 83 with permission from John Wiley and Sons. Copyright 2015 The Authors. Published by Wiley-VCH Verlag GmbH & Co. KGaA, Weinheim. (C top) A gradient magnetic field can induce magnetotaxis along the magnetic gradient. At position 0, 1 cm away from the magnet, motion and directionality increased in comparison to position 1, 3, 5 cm away from the magnet; however, at position 1 with added H_2O_2 speeds increased with respect to the second graph. (C bottom) Homogeneous magnetic fields were used to navigate nanomotors in the presence of fuel. Images 1 to 4 show that they can be guided along a distinct path. Adapted from ref 87 with permission from John Wiley and Sons. Copyright 2016 Wiley-VCH Verlag GmbH & Co. KGaA, Weinheim. (D) Sustained motion was obtained by encapsulating a enzymatic network inside stomatocytes, which is shown in the middle. The graph below shows that the speed was constant over time and thus not dependent on fuel concentration. Adapted with permission from ref 88. Copyright 2016 American Chemical Society.

biocompatibility. Restarting the motor means getting rid of all the chemicals added for inhibition, which is time-consuming and in biological context not possible. With this in mind, finding a method to incorporate the ability for nanomotors to respond to its environment without altering its structure or its catalytic activity remains a challenging task. Here we discuss our attempts to make adaptive systems by gaining control over motion and directionality.

4.1. Control over Motion. Our strategy to gain control over motion is by incorporating stimuli responsive units onto the stomatocytes opening, which allows reversible opening and closing of the "molecular valve" upon, for example, a temperature stimulus. This will lead to a cut off of the fuel supply and thus stop the motor from moving autonomously. This motion-controlled system is based on the integration of a temperature-responsive poly(*N*-isopropylacrylamide) (PNI-

DOI: 10.1021/acs.biomac.8b01673
Biomacromolecules 2019, 20, 1135−1145

PAM) brush onto the stomatocyte nanomotor surface that was grown onto the motor's surface using surface-initiated atom transfer radical polymerization (SI-ATRP).[77] PNIPAM is a temperature-responsive polymer with a lower critical solution temperature (LCST) of around 35 °C.[78] Above this LCST, PNIPAM undergoes a transformation from hydrophilic to hydrophobic that leads to a collapsed, coiled state of the polymer, forming a hydrophobic layer on top of the stomatocyte opening. The hydrophobic layer prevents access of the fuel to the nanomotor cavity, thereby ceasing their propulsion (Figure 4A). Turning the motor "on" and "off" is completely reversible and does not affect the motion behavior significantly. PNIPAM functionalized nanomotors exhibit only slightly lower speeds than the nonfunctionalized nanomotors. This might be due to its increased size or decreased diffusion through the PNIPAM brush, which lowers the access of fuel inside the nanomotor even in its hydrophilic state. At higher temperatures, however, the propulsion diminished to a level that is almost as low as Brownian motion indicating successful functioning of the thermoresponsive brake system.

4.2. Control over Directionality. While achieving control over the motion is crucial for autonomous complex systems, control over directionality is of great significance especially for potential biomedical applications. An example is active drug delivery toward tumor cells that overproduce signaling molecules, i.e., hydrogen peroxide, that fuel the motion of the motor.[79] Excellent research has shown directional control of nano/micromotors by guiding them to the desired locations. Such a control is usually a response of the motors toward external stimulus such as temperature,[80] light,[81] concentration gradients,[82,83] and magnetic fields.[84]

Again, nature is a great inspiration when it comes to directional movement. Bacteria, amoebas, and neutrophils sense substrate concentration gradients and accordingly navigate toward them.[85] Scientists have shown chemotaxis of various motors[82] or even single enzymes.[86] Chemotactic behavior toward high fuel concentration was also observed for the platinum loaded stomatocytes.[83] Different models were used to study the chemotactic behavior of platinum loaded stomatocytes, including static, dynamic and cell models. In the static and dynamic fluidic models, directionality toward higher fuel concentrations was observed even at concentrations as low as 0.5% hydrogen peroxide. The nanomotors showed chemotactic behavior along the fuel gradient as well as increased velocities at higher concentrations. Hydrogen peroxide excreting neutrophils were used as cell-model. Neutrophils in cell culture substrate were placed in the middle of a Petri dish containing a nanomotor solution. The nanomotors showed directional movement toward the hydrogen peroxide excreting cells. A decrease in directionality and speed was observed for positions further away from the fuel source (Figure 4B). It was hypothesized that the chemotactic directional control in movement was due to nanomotors developing higher speeds at higher fuel concentrations, thus traveling longer distances.

Another method to control motion is by the use of external magnetic fields, which allows a long-range directional control. Nickel loaded nanomotors are susceptible to magnetic fields due to their ferromagnetic behavior resulting in magnetotaxis.[87] Magnetic locomotion can be achieved by magnetic gradients while homogeneous fields can be used as navigation in the presence of fuel (Figure 4C). A gradient is established by using only one NdFeB magnet at the desired location, whereas homogeneous magnetic fields are applied by sandwiching the sample in between two magnets. Nanomotors encapsulating both platinum and nickel are catalytically powered in the presence of hydrogen peroxide as well as magnetic field and can be operated in dual propulsion mode. Adding hydrogen peroxide in combination with the magnetic gradient resulted in increased velocity and directionality. Magnetic locomotion is thus possible using magnetic gradients and can be enhanced by adding fuel. A collagen network loaded with HeLa cells was used as a tissue mimic to test transportation abilities of the nanomotors using magnetic locomotion. The nanomotors were guided through the gel network toward a cell via the magnetic gradient. Removing the homogeneous magnetic field resulted in dispersive movement.

4.3. Adaptive System with Feedback Control. The nanomotors based on platinum nanoparticles and the GOx/Cat cascade were relatively simple nanomotor systems and an early attempt to increase biocompatibility. However, biological systems are using metabolic pathways, out-of-equilibrium enzymatic networks with integrated feedback loops, which allow adaptation in response to changes in the environment. We have implemented this bioinspired concept and incorporated an entire glycolysis inspired metabolic pathway inside the stomatocytes to generate adaptive nanomotors with sustained autonomous movement.[88] This system can sense and adapt to the chemical environment and the presence of available fuel.

An enzymatic reaction network that is able to convert naturally present substrates into molecular oxygen was rationally designed. This enzymatic network consists of four metabolic modules, working together for tunable and sustained output. The first "activation module" acts as activation and regulation of the enzyme cycles by the conversion of ATP. The next cycle is responsible for the generation of β-nicotinamide adenine dinucleotide (β-NADH), which is consumed in the third cycle to produce hydrogen peroxide. Finally, the last cycle containing Cat will decompose hydrogen peroxide into water and oxygen and is thus the motor of the system. This enzymatic reaction network was encapsulated in the cavity of PEG-PS stomatocytes and their motion was further analyzed in the presence of glucose as fuel. At 10 mM glucose, the motors speed output stayed constant even after 180 min, highlighting the ability of this network in sustaining its output through extended periods of time by regulating fuel consumption (Figure 4D). The network output was also tuned by changing ATP concentration, because ATP determines the concentration of β-NADH and thus the consequent hydrogen peroxide production. The capability of this enzymatic network to maintain a fixed motor speed output during glucose consumption and the possibility of tuning this output by controlling the speed of certain cycles in the network is unique and advantageous.

In this case, the protective element and the confinement effect of the stomatocyte nanomotor was highlighted by showing its functioning in complex media, human blood serum (HBS). HBS contains many different proteins and enzymes, among which is catalase. When hydrogen peroxide is not produced in the cavity, but in bulk, it is converted by free catalase present in the medium. As a result, the hydrogen peroxide concentration is lowered to such an extent that the entrapped catalase cannot induce any propulsion anymore. In HBS, motion of stomatocytes was maintained and was unaffected by the media. This is an important aspect when considering the use of this system in biological context.

DOI: 10.1021/acs.biomac.8b01673
Biomacromolecules 2019, 20, 1135−1145

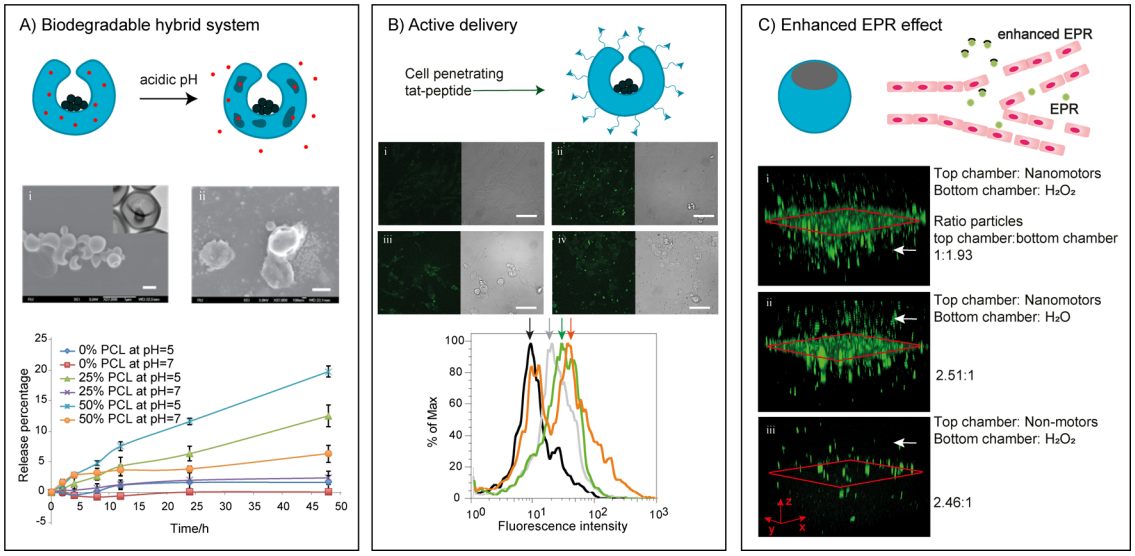

Figure 5. (A) Biodegradable hybrid nanomotor system, stomatocytes made from mixture of PEG-PCL and PEG-PS. (i) Cryo-SEM image of nonbiodegradable PEG-PS stomatocytes. (ii) Cryo-SEM image of hybrid biodegradable PEG-PS:PEG-PCL stomatocytes after pore formation. The bottom graph shows increased release of cargo for vesicles that have a higher percentage of PEG-PCL at low pH. Adapted with permission from ref 66. Copyright 2017 American Chemical Society. (B) Stomatocyte functionalized with cell penetration tat-peptide. Fluorescent and bright-field image of cell uptake for nonactive (i) and active (ii) particles and nonactive tat-functionalized (iii) and active tat-functionalized (iv) particles and the corresponding graph showing fluorescent intensity. Active tat-functionalized particles showed increased uptake over nonactive nonfunctionalized particles. Adapted with permission from ref 94. Copyright 2017 The Royal Society of Chemistry. (C) Polymersome nanomotors show enhanced EPR effect. Fluorescent confocal z-stacks show accumulation of active particles in the hydrogen peroxide rich bottom chamber, while this is to a lesser extent with water or with nonactive particles. Adapted from ref 97 with permission from John Wiley and Sons. Copyright 2018 Wiley-VCH Verlag GmbH & Co. KGaA, Weinheim.

5. BIOMEDICAL APPLICATIONS

Many of the nanomotor designs have been developed with the idea of using them for biomedical applications, such as drug delivery,[15,83] organelle mimics,[89−91] and cargo transporters in medical devices.[92,93] One of the greatest challenge is, however, the realization of a nanometer scale transporter with controlled size, shape, and suitable design to facilitate these applications. In particular, the biodegradability and biocompatibility of the transporter as well as the available fuels in biological systems. Furthermore, the nanostructures should be able to capture cargo, transport and release it at the desired location, which desirably would be inside cells for drug delivery purposes. We already discussed the formation of biocompatible/degradable structures, catalysts and fuels. The next step is to translate this to biomedical applications, for which the motors should be able to release cargo and to actively find the desired location.

5.1. Release of Cargo. A hydrophilic cargo drug can be captured inside the hydrophilic core of the polymersomes, after which it can be transformed into a nanomotor carrying this cargo in the inner compartment. To be able to release this cargo, the nanomotor membrane should be degradable. This can be done by incorporating biodegradable building blocks such as PCL as hydrophobic part to make mixed PEG-PCL/PEG-PS stomatocyte structures. Incorporation of up to 75% PEG-*b*-PCL maintained the stomatocyte morphology and did not affect the speed of the motor.[66] The PEG-*b*-PCL formed domains in the bilayer vesicle at percentages higher than 50% due to its semicrystallinity. This is advantageous, because PCL degrades at low pH, and resulted in the formation of large pores in the stomatocytes, which enabled release of cargo. Higher percentages of PCL showed increased release of cargo at pH 5 (Figure 5A). In vitro experiments showed that particles were taken up by HeLa cells and subsequently released their cargo as a response to the local low pH environment. The reference sample, consisting of non-biodegradable PEG-PS nanomotors, did not release their cargo as can be seen by the presence of fluorescent spots instead of the homogeneously spread doxorubicin with the partly biodegradable system.[94] The same was observed for nanomotors having a disulfide bridge in between the hydrophilic and hydrophobic part of the polymers.[95] In the presence of reducing agent glutathione, which is also present in cells, the nanomotors cease their motion and release the drug upon complete destruction of their structure. In vitro, this resulted in a homogeneous diffusion of doxorubicin for the degradable motors, while the motors lacking the disulfide bridge were staying intact.

Another approach to release cargo is not by destroying the stomatocytes, but by changing their morphology, which leads to a release of cargo. The cargo is in this case not loaded in the inner polymersome core, but inside the stomatocyte cavity. Here, the cargo is in contact with the outer environment and can be released by opening the stomatocyte neck. Manipulation of the shape can be done by magnetic fields, because polystyrene is diamagnetic and it has a high anisotropic susceptibility in high magnetic fields.[54] When a magnetic field was applied to a stomatocyte solution containing a plasticizing organic solvent, a deformation was observed from an overall spherical stomatocyte structure to an elongated stomatocyte. Such a deformation is a result of the phenyl groups present in the PS backbone, which has a preference to align perpendicular to the applied magnetic field. Upon applying a magnetic field, first, the stomatocytes aligned because of the anisotropic distribution of the polymer orientations. Subsequently, the polymers itself aligned perpendicular to the magnetic field, inducing a change in morphology. This alignment resulted in a

DOI: 10.1021/acs.biomac.8b01673
Biomacromolecules 2019, 20, 1135−1145

more stretched, elongated morphology and opened up the neck. The morphological change is completely reversible and dependent on the magnetic field strength, stronger fields result in a larger opening. This method allows for cargo to be captured and released at will and results in a more subtle release than the destruction of the whole system. However, the drawback of this system is the use of high magnetic fields.

5.3. Active Delivery. The next step is to obtain active delivery of the cargo to the desired location. Despite the disadvantages, the vast majority of drug delivery vehicles and their research is focused on passive delivery, which is slow and nonspecific. Enhanced uptake was already observed for nonfunctionalized active particles (nanomotors in the presence of fuel) compared to nonactive particles (nanomotors without fuel) due to a higher chance of interaction (Figure 5Bi-ii). We functionalized stomatocyte nanomotors with a cell penetrating peptide, trans-activator of transcription (tat),[94] which ensured active uptake of our nanomotors into the cells. Cell experiments showed enhanced uptake of tat-functionalized nanomotors compared to nonfunctionalized nanomotors, due not only to their cell penetrating abilities but also to their associated motion (Figure 5Biii-iv). Having both an active system as well as an active uptake mechanism will result in fast and efficient cell penetration. This approach will ensure uptake into cells, yet, reaching the diseased cells is a different problem. Until now, drug delivery is mostly passive utilizing the enhanced permeation and retention (EPR) effect. This effect is a result of the leaky blood vessels around a tumor which enhances the entry and accumulation of nutrients as well as drugs.[96] We investigated an enhanced EPR effect to reach cancer tissue by the exploitation of the nanomotors chemotactic behavior toward higher fuel concentrations,[97] as explained earlier. A model was made from a double-layer microslide consisting of an upper and bottom chamber separated by a porous membrane seeded with endothelial cells. The upper chamber was filled with nanomotors based on polymersomes having a platinum patch, while the bottom chamber was filled with either hydrogen peroxide or water. In the presence of hydrogen peroxide, the nanomotors accumulated twice as fast in the bottom chamber than in the presence of water. This shows that using motors as drug delivery system can result in an enhanced accumulation of the drug inside the tumor.

6. CONCLUSIONS AND FUTURE PERSPECTIVES

In this Perspective, we highlighted the crucial steps to fabricate active and adaptive locomotive systems for the use in biomedical applications and our approach to reach this goal. These include asymmetry, which is required for the formation of motors and can be obtained by the self-assembly of different amphiphilic block copolymers into different shapes, and the incorporation of enzymes or other catalysts that transforms passive vesicles into autonomous motors. We succeeded in gaining control over motion, directionality and speed and explored the possibilities of drug release and active targeting. We showed that self-assembled autonomous particles are not only capable of carrying a cargo but also move directionally in the presence of a gradient of signaling molecules produced by cells, transporting thus actively the cargo toward the cells producing fuel. Additionally the supramolecular nanomortors are interacting differently with cells compared with passive particles and are taking up faster. While blood provides good circulation of the nanocarriers at elevated speeds regardless if they are passive or active, it is the interstitial tissue where locomotive particles can help to facilitate crossing of the last barriers, which is a challenge in current delivery applications. Additionally, supramolecular nanomorors were demonstrated to facilitate enhanced EPR effect, spreading faster toward the signaling molecules compared to passive carriers.

Despite all the progress in the micro and nanomotor field during the past years, there are still challenges to overcome and questions to be answered, both regarding their mechanism of motion and movement in crowded environment but also toward their feasibility for applications in the biomedical field. This goal is coming slowly closer; however, most of the nanomotor systems are not at all or only partly biocompatible, utilizing toxic fuels for propulsion. The challenge is thus to construct fully biocompatible and biodegradable motors that can move directionally via chemotaxis in complex and crowded biological environments and at biological relevant fuel concentrations which are much lower than what has been studied so far. Another challenge is to have all these functionalities combined in one active delivery system while moving in biological fluids. Until now, most research has been done in water or buffer. However, bodily fluids have a complex composition of many different substituents that will affect motion but could also affect other functionalities such as targeting.

Another question that remains is a more fundamental one. What is the exact underlying mechanism of motion and how can we control the motion, directionality, and speed at the nanoscale in complex environments? This depends on different aspects of the motors, such as size and the materials it is made of. This is an experimentally difficult question when dealing with nanomotors, because most of the analysis techniques, such as light scattering, are indirect. This challenge makes it even more interesting to answer this question. When the mechanism of motion is clear and completely understood, we can more easily manipulate the system and this will help overcome challenges and reach goals that are still ahead. The recently published hydrogel micromotors from our group will be used for this goal, to gain more insight in the mechanism of motion and how to control this.

AUTHOR INFORMATION

Corresponding Author

*D. A. Wilson. E-mail: d.wilson@science.ru.nl.

ORCID

Daniela A. Wilson: 0000-0002-8796-2274

Author Contributions

‡These authors contributed equally.

Funding

NWO Chemische Wetenschappen VIDI Grant 723.015.001. ERC Starting Grant 307679 StomaMotors. Ministry of Education, Culture and Science (Gravitation program 024.001.035).

Notes

The authors declare no competing financial interest.

ACKNOWLEDGMENTS

We acknowledge financial support from the NWO Chemische Wetenschappen VIDI Grant 723.015.001. D.A.W. acknowledges support from the ERC Starting Grant 307679 StomaMotors and Ministry of Education, Culture and Science (Gravitation program 024.001.035). We thank all members of

DOI: 10.1021/acs.biomac.8b01673
Biomacromolecules 2019, 20, 1135−1145

the Systems Chemistry department for their contributions to this field and their valuable discussions.

■ ABBREVIATIONS

PEG, poly(ethylene glycol); PBD, polybutadiene; PS, polystyrene; PCL, poly(ε-caprolactone); PLA, polylactide; PDLLA, poly(D,L-lactide); ATRP, atom transfer radical polymerization; ROP, ring opening polymerization; PEGDA, poly(ethylene glycol) diacrylate; GOx, glucose oxidase; Cat, catalase; cryo-TEM, cryo-transmission electron microscopy; EDX, energy dispersive X-ray spectroscopy; cryo-SEM, cryo-scanning electron microscopy; PNIPAM, poly(*N*-isopropylacrylamide); SI-ATRP, surface-initiated atom transfer radical polymerization; LCST, lower critical solution temperature; β-NADH, β-nicotinamide adenine dinucleotide; HBS, human blood serum; tat, trans-activator of transcription; EPR, enhanced permeation and retention.

■ REFERENCES

(1) Nissen, P.; Hansen, J.; Ban, N.; Moore, P. B.; Steitz, T. A. The Structural Basis of Ribosome Activity in Peptide Bond Synthesis. *Science* **2000**, *289* (5481), 920−930.

(2) Vale, R. D.; Funatsu, T.; Pierce, D. W.; Romberg, L.; Harada, Y.; Yanagida, T. Direct observation of single kinesin molecules moving along microtubules. *Nature* **1996**, *380* (6573), 451−453.

(3) Giorgio, V.; von Stockum, S.; Antoniel, M.; Fabbro, A.; Fogolari, F.; Forte, M.; Glick, G. D.; Petronilli, V.; Zoratti, M.; Szabó, I.; Lippe, G.; Bernardi, P. Dimers of mitochondrial ATP synthase form the permeability transition pore. *Proc. Natl. Acad. Sci. U. S. A.* **2013**, *110* (15), 5887−5892.

(4) Kulago, A. A.; Mes, E. M.; Klok, M.; Meetsma, A.; Brouwer, A. M.; Feringa, B. L. Ultrafast Light-Driven Nanomotors Based on an Acridane Stator. *J. Org. Chem.* **2010**, *75* (3), 666−679.

(5) Kudernac, T.; Ruangsupapichat, N.; Parschau, M.; Macia, B.; Katsonis, N.; Harutyunyan, S. R.; Ernst, K.-H.; Feringa, B. L. Electrically driven directional motion of a four-wheeled molecule on a metal surface. *Nature* **2011**, *479* (7372), 208−211.

(6) Cnossen, A.; Pijper, D.; Kudernac, T.; Pollard, M. M.; Katsonis, N.; Feringa, B. L. A Trimer of Ultrafast Nanomotors: Synthesis, Photochemistry and Self-Assembly on Graphite. *Chem. - Eur. J.* **2009**, *15* (12), 2768−2772.

(7) Feringa, B. L.; van Delden, R. A.; Koumura, N.; Geertsema, E. M. Chiroptical Molecular Switches. *Chem. Rev.* **2000**, *100* (5), 1789−1816.

(8) Kelly, T. R.; Tellitu, I.; Sestelo, J. P. Search of Molecular Ratchets. *Angew. Chem., Int. Ed. Engl.* **1997**, *36* (17), 1866−1868.

(9) Demirok, U. K.; Laocharoensuk, R.; Manesh, K. M.; Wang, J. Ultrafast Catalytic Alloy Nanomotors. *Angew. Chem., Int. Ed.* **2008**, *47* (48), 9349−9351.

(10) Laocharoensuk, R.; Burdick, J.; Wang, J. Carbon-Nanotube-Induced Acceleration of Catalytic Nanomotors. *ACS Nano* **2008**, *2* (5), 1069−1075.

(11) Garcia-Gradilla, V.; Orozco, J.; Sattayasamitsathit, S.; Soto, F.; Kuralay, F.; Pourazary, A.; Katzenberg, A.; Gao, W.; Shen, Y.; Wang, J. Functionalized Ultrasound-Propelled Magnetically Guided Nanomotors: Toward Practical Biomedical Applications. *ACS Nano* **2013**, *7* (10), 9232−9240.

(12) Liu, R.; Sen, A. Autonomous Nanomotor Based on Copper−Platinum Segmented Nanobattery. *J. Am. Chem. Soc.* **2011**, *133* (50), 20064−20067.

(13) Kline, T. R.; Paxton, W. F.; Mallouk, T. E.; Sen, A. Catalytic Nanomotors: Remote-Controlled Autonomous Movement of Striped Metallic Nanorods. *Angew. Chem.* **2005**, *117* (5), 754−756.

(14) Schattling, P.; Thingholm, B.; Städler, B. Enhanced Diffusion of Glucose-Fueled Janus Particles. *Chem. Mater.* **2015**, *27* (21), 7412−7418.

(15) Xuan, M.; Shao, J.; Lin, X.; Dai, L.; He, Q. Self-Propelled Janus Mesoporous Silica Nanomotors with Sub-100 nm Diameters for Drug Encapsulation and Delivery. *ChemPhysChem* **2014**, *15* (11), 2255−2260.

(16) Ashton, P. R.; Ballardini, R.; Balzani, V.; Baxter, I.; Credi, A.; Fyfe, M. C. T.; Gandolfi, M. T.; Gómez-López, M.; Martínez-Díaz, M. V.; Piersanti, A.; Spencer, N.; Stoddart, J. F.; Venturi, M.; White, A. J. P.; Williams, D. J. Acid−Base Controllable Molecular Shuttles. *J. Am. Chem. Soc.* **1998**, *120* (46), 11932−11942.

(17) Wilson, D. A.; Nolte, R. J. M.; van Hest, J. C. M. Entrapment of Metal Nanoparticles in Polymer Stomatocytes. *J. Am. Chem. Soc.* **2012**, *134* (24), 9894−9897.

(18) Burdick, J.; Laocharoensuk, R.; Wheat, P. M.; Posner, J. D.; Wang, J. Synthetic Nanomotors in Microchannel Networks: Directional Microchip Motion and Controlled Manipulation of Cargo. *J. Am. Chem. Soc.* **2008**, *130* (26), 8164−8165.

(19) Soto, F.; Wagner, G. L.; Garcia-Gradilla, V.; Gillespie, K. T.; Lakshmipathy, D. R.; Karshalev, E.; Angell, C.; Chen, Y.; Wang, J. Acoustically propelled nanoshells. *Nanoscale* **2016**, *8* (41), 17788−17793.

(20) Manesh, K. M.; Cardona, M.; Yuan, R.; Clark, M.; Kagan, D.; Balasubramanian, S.; Wang, J. Template-Assisted Fabrication of Salt-Independent Catalytic Tubular Microengines. *ACS Nano* **2010**, *4* (4), 1799−1804.

(21) Wang, W.; Duan, W.; Sen, A.; Mallouk, T. E. Catalytically powered dynamic assembly of rod-shaped nanomotors and passive tracer particles. *Proc. Natl. Acad. Sci. U. S. A.* **2013**, *110* (44), 17744−17749.

(22) Koumura, N.; Zijlstra, R. W. J.; van Delden, R. A.; Harada, N.; Feringa, B. L. Light-driven monodirectional molecular rotor. *Nature* **1999**, *401* (6749), 152−155.

(23) Van Delden, R. A.; Ter Wiel, M. K.; Pollard, M. M.; Vicario, J.; Koumura, N.; Feringa, B. L. Unidirectional molecular motor on a gold surface. *Nature* **2005**, *437* (7063), 1337.

(24) Eelkema, R.; Pollard, M. M.; Vicario, J.; Katsonis, N.; Ramon, B. S.; Bastiaansen, C. W.; Broer, D. J.; Feringa, B. L. Molecular machines: nanomotor rotates microscale objects. *Nature* **2006**, *440* (7081), 163.

(25) Lin, C.; Ke, Y.; Liu, Y.; Mertig, M.; Gu, J.; Yan, H. Functional DNA Nanotube Arrays: Bottom-Up Meets Top-Down. *Angew. Chem., Int. Ed.* **2007**, *46* (32), 6089−6092.

(26) Cheng, J. Y.; Ross, C. A.; Smith, H. I.; Thomas, E. L. Templated self-assembly of block copolymers: top-down helps bottom-up. *Adv. Mater.* **2006**, *18* (19), 2505−2521.

(27) Wu, Y.; Lin, X.; Wu, Z.; Möhwald, H.; He, Q. Self-propelled polymer multilayer Janus capsules for effective drug delivery and light-triggered release. *ACS Appl. Mater. Interfaces* **2014**, *6* (13), 10476−10481.

(28) Hawthorne, M. F.; Zink, J. I.; Skelton, J. M.; Bayer, M. J.; Liu, C.; Livshits, E.; Baer, R.; Neuhauser, D. Electrical or Photocontrol of the Rotary Motion of a Metallacarborane. *Science* **2004**, *303* (5665), 1849−1851.

(29) Badjić, J. D.; Balzani, V.; Credi, A.; Silvi, S.; Stoddart, J. F. A Molecular Elevator. *Science* **2004**, *303* (5665), 1845−1849.

(30) Wilson, D. A.; Nolte, R. J. M.; van Hest, J. C. M. Autonomous movement of platinum-loaded stomatocytes. *Nat. Chem.* **2012**, *4* (4), 268−274.

(31) Abdelmohsen, L. K. E. A.; Rikken, R. S. M.; Christianen, P. C. M.; van Hest, J. C. M.; Wilson, D. A. Shape characterization of polymersome morphologies via light scattering techniques. *Polymer* **2016**, *107*, 445−449.

(32) Rikken, R. S. M.; Kerkenaar, H. H. M.; Nolte, R. J. M.; Maan, J. C.; van Hest, J. C. M.; Christianen, P. C. M.; Wilson, D. A. Probing morphological changes in polymersomes with magnetic birefringence. *Chem. Commun.* **2014**, *50* (40), 5394−5396.

(33) Keller, S.; Teora, S. P.; Hu, G. X.; Nijemeisland, M.; Wilson, D. A. High-Throughput Design of Biocompatible Enzyme-Based Hydrogel Microparticles with Autonomous Movement. *Angew. Chem., Int. Ed.* **2018**, *57* (31), 9814−9817.

DOI: 10.1021/acs.biomac.8b01673
Biomacromolecules 2019, 20, 1135−1145

(34) Abdelmohsen, L. K. E. A.; Peng, F.; Tu, Y.; Wilson, D. A. Micro- and nano-motors for biomedical applications. *J. Mater. Chem. B* **2014**, *2* (17), 2395−2408.
(35) Wong, F.; Dey, K. K.; Sen, A. Synthetic Micro/Nanomotors and Pumps: Fabrication and Applications. *Annu. Rev. Mater. Res.* **2016**, *46* (1), 407−432.
(36) Karshalev, E.; Esteban-Fernández de Ávila, B.; Wang, J. Micromotors for "Chemistry-on-the-Fly. *J. Am. Chem. Soc.* **2018**, *140* (11), 3810−3820.
(37) Cheng, C.; Stoddart, J. F. Wholly Synthetic Molecular Machines. *ChemPhysChem* **2016**, *17* (12), 1780−1793.
(38) Kassem, S.; van Leeuwen, T.; Lubbe, A. S.; Wilson, M. R.; Feringa, B. L.; Leigh, D. A. Artificial molecular motors. *Chem. Soc. Rev.* **2017**, *46* (9), 2592−2621.
(39) Petrosko, S. H.; Johnson, R.; White, H.; Mirkin, C. A. Nanoreactors: Small Spaces, Big Implications in Chemistry. *J. Am. Chem. Soc.* **2016**, *138* (24), 7443−7445.
(40) Deraedt, C.; Astruc, D. Supramolecular nanoreactors for catalysis. *Coord. Chem. Rev.* **2016**, *324*, 106−122.
(41) Marguet, M.; Bonduelle, C.; Lecommandoux, S. Multi-compartmentalized polymeric systems: towards biomimetic cellular structure and function. *Chem. Soc. Rev.* **2013**, *42* (2), 512−529.
(42) Abdelmohsen, L. K. E. A.; Nijemeisland, M.; Pawar, G. M.; Janssen, G.-J. A.; Nolte, R. J. M.; van Hest, J. C. M.; Wilson, D. A. Dynamic Loading and Unloading of Proteins in Polymeric Stomatocytes: Formation of an Enzyme-Loaded Supramolecular Nanomotor. *ACS Nano* **2016**, *10* (2), 2652−2660.
(43) Lee, J. S.; Feijen, J. Polymersomes for drug delivery: Design, formation and characterization. *J. Controlled Release* **2012**, *161* (2), 473−483.
(44) Ghoroghchian, P. P.; Frail, P. R.; Susumu, K.; Blessington, D.; Brannan, A. K.; Bates, F. S.; Chance, B.; Hammer, D. A.; Therien, M. J. Near-infrared-emissive polymersomes: Self-assembled soft matter for in vivo optical imaging. *Proc. Natl. Acad. Sci. U. S. A.* **2005**, *102* (8), 2922−2927.
(45) Martino, C.; Kim, S.-H.; Horsfall, L.; Abbaspourrad, A.; Rosser, S. J.; Cooper, J.; Weitz, D. A. Protein Expression, Aggregation, and Triggered Release from Polymersomes as Artificial Cell-like Structures. *Angew. Chem., Int. Ed.* **2012**, *51* (26), 6416−6420.
(46) Liu, F.; Eisenberg, A. Preparation and pH Triggered Inversion of Vesicles from Poly(acrylic Acid)-block-Polystyrene-block-Poly(4-vinyl Pyridine). *J. Am. Chem. Soc.* **2003**, *125* (49), 15059−15064.
(47) Adams, D. J.; Adams, S.; Atkins, D.; Butler, M. F.; Furzeland, S. Impact of mechanism of formation on encapsulation in block copolymer vesicles. *J. Controlled Release* **2008**, *128* (2), 165−170.
(48) Abdelmohsen, L. K. E. A.; Williams, D. S.; Pille, J.; Ozel, S. G.; Rikken, R. S. M.; Wilson, D. A.; van Hest, J. C. M. Formation of Well-Defined, Functional Nanotubes via Osmotically Induced Shape Transformation of Biodegradable Polymersomes. *J. Am. Chem. Soc.* **2016**, *138* (30), 9353−9356.
(49) Rikken, R. S. M.; Engelkamp, H.; Nolte, R. J. M.; Maan, J. C.; van Hest, J. C. M.; Wilson, D. A.; Christianen, P. C. M. Shaping polymersomes into predictable morphologies via out-of-equilibrium self-assembly. *Nat. Commun.* **2016**, *7*, 12606.
(50) Moughton, A. O.; Patterson, J. P.; O'Reilly, R. K. Reversible morphological switching of nanostructures in solution. *Chem. Commun.* **2011**, *47* (1), 355−357.
(51) Qin, S.; Geng, Y.; Discher, D. E.; Yang, S. Temperature-Controlled Assembly and Release from Polymer Vesicles of Poly(ethylene oxide)-block- poly(N-isopropylacrylamide). *Adv. Mater.* **2006**, *18* (21), 2905−2909.
(52) Yan, Q.; Zhou, R.; Fu, C.; Zhang, H.; Yin, Y.; Yuan, J. CO2-Responsive Polymeric Vesicles that Breathe. *Angew. Chem., Int. Ed.* **2011**, *50* (21), 4923−4927.
(53) Schmuck, C.; Rehm, T.; Klein, K.; Gröhn, F. Formation of Vesicular Structures through the Self-Assembly of a Flexible Bis-Zwitterion in Dimethyl Sulfoxide. *Angew. Chem., Int. Ed.* **2007**, *46* (10), 1693−1697.
(54) van Rhee, P. G.; Rikken, R. S. M.; Abdelmohsen, L. K. E. A.; Maan, J. C.; Nolte, R. J. M.; van Hest, J. C. M.; Christianen, P. C. M.; Wilson, D. A. Polymersome magneto-valves for reversible capture and release of nanoparticles. *Nat. Commun.* **2014**, *5*, 5010.
(55) Lecommandoux, S.; Sandre, O.; Chécot, F.; Rodriguez-Hernandez, J.; Perzynski, R. Magnetic Nanocomposite Micelles and Vesicles. *Adv. Mater.* **2005**, *17* (6), 712−718.
(56) Le Meins, J.-F.; Sandre, O.; Lecommandoux, S. Recent trends in the tuning of polymersomes' membrane properties. *Eur. Phys. J. E: Soft Matter Biol. Phys.* **2011**, *34* (2), 14.
(57) Yuan, H.; Huang, C.; Zhang, S. Dynamic shape transformations of fluid vesicles. *Soft Matter* **2010**, *6* (18), 4571−4579.
(58) Liu, G.-Y.; Chen, C.-J.; Ji, J. Biocompatible and biodegradable polymersomes as delivery vehicles in biomedical applications. *Soft Matter* **2012**, *8* (34), 8811−8821.
(59) Meng, F.; Hiemstra, C.; Engbers, G. H. M.; Feijen, J. Biodegradable Polymersomes. *Macromolecules* **2003**, *36* (9), 3004−3006.
(60) Zweers, M. L. T.; Engbers, G. H. M.; Grijpma, D. W.; Feijen, J. In vitro degradation of nanoparticles prepared from polymers based on dl-lactide, glycolide and poly(ethylene oxide). *J. Controlled Release* **2004**, *100* (3), 347−356.
(61) Che, H.; van Hest, J. C. M. Stimuli-responsive polymersomes and nanoreactors. *J. Mater. Chem. B* **2016**, *4* (27), 4632−4647.
(62) Meng, F.; Zhong, Z.; Feijen, J. Stimuli-Responsive Polymersomes for Programmed Drug Delivery. *Biomacromolecules* **2009**, *10* (2), 197−209.
(63) Onaca, O.; Enea, R.; Hughes, D. W.; Meier, W. Stimuli-Responsive Polymersomes as Nanocarriers for Drug and Gene Delivery. *Macromol. Biosci.* **2009**, *9* (2), 129−139.
(64) Checot, F.; Lecommandoux, S.; Klok, H.-A.; Gnanou, Y. From supramolecular polymersomes to stimuli-responsive nano-capsules based on poly (diene-b-peptide) diblock copolymers. *Eur. Phys. J. E: Soft Matter Biol. Phys.* **2003**, *10* (1), 25−35.
(65) Kim, K. T.; Zhu, J.; Meeuwissen, S. A.; Cornelissen, J. J. L. M.; Pochan, D. J.; Nolte, R. J. M.; van Hest, J. C. M. Polymersome Stomatocytes: Controlled Shape Transformation in Polymer Vesicles. *J. Am. Chem. Soc.* **2010**, *132* (36), 12522−12524.
(66) Tu, Y.; Peng, F.; André, A. A.; Men, Y.; Srinivas, M.; Wilson, D. A. Biodegradable hybrid stomatocyte nanomotors for drug delivery. *ACS Nano* **2017**, *11* (2), 1957−1963.
(67) Toebes, B. J.; Abdelmohsen, L. K.; Wilson, D. A. Enzyme-driven biodegradable nanomotor based on tubular-shaped polymeric vesicles. *Polym. Chem.* **2018**, *9* (23), 3190−3194.
(68) Brinkhuis, R. P.; Rutjes, F. P.; van Hest, J. C. Polymeric vesicles in biomedical applications. *Polym. Chem.* **2011**, *2* (7), 1449−1462.
(69) Seifert, U. Configurations of fluid membranes and vesicles. *Adv. Phys.* **1997**, *46* (1), 13−137.
(70) Pijpers, I. A.; Abdelmohsen, L. K.; Williams, D. S.; van Hest, J. C. Morphology under control: engineering biodegradable stomatocytes. *ACS Macro Lett.* **2017**, *6* (11), 1217−1222.
(71) Men, Y.; Li, W.; Janssen, G.-J.; Rikken, R. S.; Wilson, D. A. Stomatocyte in Stomatocyte: A New Shape of Polymersome Induced via Chemical-Addition Methodology. *Nano Lett.* **2018**, *18* (3), 2081−2085.
(72) Kolhar, P.; Anselmo, A. C.; Gupta, V.; Pant, K.; Prabhakarpandian, B.; Ruoslahti, E.; Mitragotri, S. Using shape effects to target antibody-coated nanoparticles to lung and brain endothelium. *Proc. Natl. Acad. Sci. U. S. A.* **2013**, *110* (26), 10753−10758.
(73) Sorrenti, A.; Leira-Iglesias, J.; Markvoort, A. J.; de Greef, T. F.; Hermans, T. M. Non-equilibrium supramolecular polymerization. *Chem. Soc. Rev.* **2017**, *46* (18), 5476−5490.
(74) Meeuwissen, S. A.; Kim, K. T.; Chen, Y.; Pochan, D. J.; van Hest, J. C. Controlled shape transformation of polymersome stomatocytes. *Angew. Chem.* **2011**, *123* (31), 7208−7211.
(75) Magdanz, V.; Stoychev, G.; Ionov, L.; Sanchez, S.; Schmidt, O. G. Stimuli-Responsive Microjets with Reconfigurable Shape. *Angew. Chem., Int. Ed.* **2014**, *53* (10), 2673−2677.

DOI: 10.1021/acs.biomac.8b01673
Biomacromolecules 2019, 20, 1135−1145

(76) Ma, X.; Wang, X.; Hahn, K.; Sanchez, S. Motion Control of Urea-Powered Biocompatible Hollow Microcapsules. *ACS Nano* **2016**, *10* (3), 3597−3605.
(77) Tu, Y.; Peng, F.; Sui, X.; Men, Y.; White, P. B.; van Hest, J. C. M.; Wilson, D. A. Self-propelled supramolecular nanomotors with temperature-responsive speed regulation. *Nat. Chem.* **2016**, *9*, 480−486.
(78) Schild, H. G. Poly(N-isopropylacrylamide): experiment, theory and application. *Prog. Polym. Sci.* **1992**, *17* (2), 163−249.
(79) Wlassoff, W. A.; Albright, C. D.; Sivashinski, M. S.; Ivanova, A.; Appelbaum, J. G.; Salganik, R. I. Hydrogen peroxide overproduced in breast cancer cells can serve as an anticancer prodrug generating apoptosis-stimulating hydroxyl radicals under the effect of tamoxifen-ferrocene conjugate. *J. Pharm. Pharmacol.* **2007**, *59* (11), 1549−1553.
(80) Sanchez, S.; Ananth, A. N.; Fomin, V. M.; Viehrig, M.; Schmidt, O. G. Superfast Motion of Catalytic Microjet Engines at Physiological Temperature. *J. Am. Chem. Soc.* **2011**, *133* (38), 14860−14863.
(81) Solovev, A. A.; Smith, E. J.; Bof' Bufon, C. C.; Sanchez, S.; Schmidt, O. G. Light-Controlled Propulsion of Catalytic Micro-engines. *Angew. Chem., Int. Ed.* **2011**, *50* (46), 10875−10878.
(82) Hong, Y.; Velegol, D.; Chaturvedi, N.; Sen, A. Biomimetic behavior of synthetic particles: from microscopic randomness to macroscopic control. *Phys. Chem. Chem. Phys.* **2010**, *12* (7), 1423−1435.
(83) Peng, F.; Tu, Y.; van Hest, J. C. M.; Wilson, D. A. Self-Guided Supramolecular Cargo-Loaded Nanomotors with Chemotactic Behavior towards Cells. *Angew. Chem., Int. Ed.* **2015**, *54* (40), 11662−11665.
(84) Rikken, R. S. M.; Nolte, R. J. M.; Maan, J. C.; van Hest, J. C. M.; Wilson, D. A.; Christianen, P. C. M. Manipulation of micro- and nanostructure motion with magnetic fields. *Soft Matter* **2014**, *10* (9), 1295−1308.
(85) Kay, R. R.; Langridge, P.; Traynor, D.; Hoeller, O. Changing directions in the study of chemotaxis. *Nat. Rev. Mol. Cell Biol.* **2008**, *9* (6), 455−63.
(86) Sengupta, S.; Dey, K. K.; Muddana, H. S.; Tabouillot, T.; Ibele, M. E.; Butler, P. J.; Sen, A. Enzyme Molecules as Nanomotors. *J. Am. Chem. Soc.* **2013**, *135* (4), 1406−1414.
(87) Peng, F.; Tu, Y.; Men, Y.; van Hest, J. C. M.; Wilson, D. A. Supramolecular Adaptive Nanomotors with Magnetotaxis Behavior. *Adv. Mater.* **2017**, *29* (6), 1604996.
(88) Nijemeisland, M.; Abdelmohsen, L. K. E. A.; Huck, W. T. S.; Wilson, D. A.; van Hest, J. C. M. A Compartmentalized Out-of-Equilibrium Enzymatic Reaction Network for Sustained Autonomous Movement. *ACS Cent. Sci.* **2016**, *2* (11), 843−849.
(89) Tu, Y.; Peng, F.; Adawy, A.; Men, Y.; Abdelmohsen, L. K. E. A.; Wilson, D. A. Mimicking the Cell: Bio-Inspired Functions of Supramolecular Assemblies. *Chem. Rev.* **2016**, *116* (4), 2023−2078.
(90) Tanner, P.; Onaca, O.; Balasubramanian, V.; Meier, W.; Palivan, C. G. Enzymatic Cascade Reactions inside Polymeric Nanocontainers: A Means to Combat Oxidative Stress. *Chem. - Eur. J.* **2011**, *17* (16), 4552−4560.
(91) Schoonen, L.; van Hest, J. C. M. Compartmentalization Approaches in Soft Matter Science: From Nanoreactor Development to Organelle Mimics. *Adv. Mater.* **2016**, *28* (6), 1109−1128.
(92) Garcia, M.; Orozco, J.; Guix, M.; Gao, W.; Sattayasamitsathit, S.; Escarpa, A.; Merkoci, A.; Wang, J. Micromotor-based lab-on-chip immunoassays. *Nanoscale* **2013**, *5* (4), 1325−1331.
(93) Wang, J. Cargo-towing synthetic nanomachines: Towards active transport in microchip devices. *Lab Chip* **2012**, *12* (11), 1944−1950.
(94) Peng, F.; Tu, Y.; Adhikari, A.; Hintzen, J. C. J.; Lowik, D. W. P. M.; Wilson, D. A. A peptide functionalized nanomotor as an efficient cell penetrating tool. *Chem. Commun.* **2017**, *53* (6), 1088−1091.
(95) Tu, Y.; Peng, F.; White, P. B.; Wilson, D. A. Redox-Sensitive Stomatocyte Nanomotors: Destruction and Drug Release in the Presence of Glutathione. *Angew. Chem., Int. Ed.* **2017**, *56* (26), 7620−7624.
(96) Fang, J.; Nakamura, H.; Maeda, H. The EPR effect: Unique features of tumor blood vessels for drug delivery, factors involved, and limitations and augmentation of the effect. *Adv. Drug Delivery Rev.* **2011**, *63* (3), 136−151.
(97) Peng, F.; Men, Y.; Tu, Y.; Chen, Y.; Wilson, D. A. Nanomotor-Based Strategy for Enhanced Penetration across Vasculature Model. *Adv. Funct. Mater.* **2018**, *28*, 1706117.

DOI: 10.1021/acs.biomac.8b01673
Biomacromolecules 2019, 20, 1135−1145